
This is an electronic reprint of the original article.
This reprint may differ from the original in pagination and typographic detail.

Tofighi-Milani, Mahyar; Fattaheian-Dehkordi, Sajjad; Lehtonen, Matti
Electrolysers: A Review on Trends, Electrical Modeling, and Their Dynamic Responses

Published in:
IEEE Access

DOI:
[10.1109/ACCESS.2025.3546546](https://doi.org/10.1109/ACCESS.2025.3546546)

E-pub ahead of print: 01/01/2025

Document Version
Publisher's PDF, also known as Version of record

Published under the following license:
CC BY

Please cite the original version:
Tofighi-Milani, M., Fattaheian-Dehkordi, S., & Lehtonen, M. (2025). Electrolysers: A Review on Trends, Electrical Modeling, and Their Dynamic Responses. *IEEE Access*, 13. Advance online publication. <https://doi.org/10.1109/ACCESS.2025.3546546>

This material is protected by copyright and other intellectual property rights, and duplication or sale of all or part of any of the repository collections is not permitted, except that material may be duplicated by you for your research use or educational purposes in electronic or print form. You must obtain permission for any other use. Electronic or print copies may not be offered, whether for sale or otherwise to anyone who is not an authorised user.

TOPICAL REVIEW

Electrolysers: A Review on Trends, Electrical Modeling, and Their Dynamic Responses

MAHYAR TOFIGHI-MILANI^{ID}, (Student Member, IEEE),

SAJJAD FATTAHEIAN-DEHKORDI^{ID}, (Member, IEEE), AND MATTI LEHTONEN^{ID}

Department of Electrical Engineering and Automation, Aalto University, 02150 Espoo, Finland

Corresponding author: Sajjad Fattaheian-Dehkordi (sajjad.fattaheiandehkordi@aalto.fi)

ABSTRACT The global movement towards high integration of renewable energy sources into power systems to combat climate change underscores the importance of clean energy sources in sustainable development of future energy systems. Simultaneously, hydrogen is gaining prominence as a clean fuel, particularly in sectors like industry and transportation. However, the intermittent nature of renewable energies poses challenges for demand-supply balance and grid stability, necessitating efficient storage solutions. Additionally, the hydrogen economy introduces a new dimension to the challenge of power system balance management. In terms of electrical modeling, particularly for power system stability analysis, dynamic models of electrolysers are essential. Water electrolysis, powered by surplus renewable energy, has emerged as a promising method for hydrogen production, fostering advancements in sustainable energy practices. This paper provides an overview of electrolysis, exploring the electrical behavior of Alkaline, proton exchange membrane, and solid oxide electrolysers, while also categorizing them from a modelling perspective. Respectively, it examines the electrical modeling of electrolysers, encompassing three main formats: electrical equivalent circuit (EEC), mathematical formulation (MF), and block diagram (BD) presentation. Additionally, this paper investigates the dynamic responses of Alkaline and proton exchange membrane electrolysers, identified as the most suitable types for integration into power system dynamic studies. Through a review of existing literature and categorization of models, this paper aims to offer a comprehensive understanding of electrolyser behavior and dynamics in operation of power grids.

INDEX TERMS Alkaline electrolyser, proton exchange membrane electrolyser, solid oxide electrolyser, electrolyser modeling, electrical equivalent circuit, dynamic response of electrolysers.

NOMENCLATURE

Abbreviations

RES	Renewable energy sources.
AE	Alkaline electrolyser.
PEME	Proton exchange membrane electrolyser.
SOE	Solid oxide electrolyser.
EEC	Electrical equivalent circuit.
MF	Mathematical formulation.
BD	Block diagram.
DLE	Double layer effect.

Parameters

V_{cell}, I_{cell}	Terminal voltage and current of an electrolyser cell.
V_{rev}	Reversible voltage.
V_{ohm}	Ohmic voltage drop.
V_{act}	Activation overvoltage.
$V_{act,a}/V_{act,c}$	Activation overvoltage in anode/cathode.
V_{con}	Concentration overvoltage.
$V_{con,a}/V_{con,c}$	concentration overvoltage in anode/cathode.
I_{act}	Activation current.
$I_{act,a}/I_{act,c}$	Activation current of anode/cathode.
R_{ohm}	Ohmic resistance.
R_{act}	Activation resistance.

The associate editor coordinating the review of this manuscript and approving it for publication was Jahangir Hossain^{ID}.

$R_{act,a}/R_{act,c}$	Activation resistance of anode/cathode.	l_a, l_m, l_c, l_e	The anode/membrane/cathode/electrolyte thickness.
R_{con}	Concentration resistance.	$\sigma_a/\sigma_m/\sigma_c$	The conductivity of the anode/membrane/cathode.
C_{act}	Activation capacitance.		
$C_{act,a}/C_{act,c}$	Activation capacitance of anode/cathode.	$\rho_a/\rho_e/\rho_c$	Resistivity of anode/electrolyte/cathode.
C_{dle}	The capacitance modeling for double layer effect.	$\sigma_a/\sigma_e/\sigma_c$	The conductivity of the anode/electrolyte/cathode.
L_{act}	Inductance modeling of activation phenomenon.	$r_{a1}^{ohm}, r_{e1}^{ohm}, r_{c1}^{ohm}, r_{a2}^{ohm}, r_{e2}^{ohm}, r_{c2}^{ohm}$	Constant coefficients related to the ohmic resistance of the anode/electrolyte/cathode.
Z_{con}	Impedance modeling of concentration phenomenon.		
F	Faraday's constant.	$R_{ohm}^{e,b}$	Ohmic resistance of electrolyte due to bubbles.
R	Universal ideal gas constant.	$R_{ohm}^{e,bf}$	Bubble-free electrolyte resistance.
n	Number of the electron moles transferred per hydrogen mole.	$\sigma_{e,bf}$	Bubble-free electrolyte conductivity.
ΔG	Change in Gibbs free energy of reaction.	$l_{a,m}, l_{c,m}$	Anode-membrane and the cathode-membrane distances.
P, T	The operating pressure and temperature of the electrolyser.	A_{eff}	Effective electrode surface.
P^{std}, T^{std}	Standard pressure and temperature.	t	Time.
V_{stp}^{rev}	Reversible voltage at standard conditions.	L^{-1}	Inverse Laplace transform operator.
P_{H_2}/P_{O_2}	Partial pressure of hydrogen/oxygen.	s	Complex frequency in Laplace transform.
$P_{H_2O}/P_{H_2O}^0$	Partial pressure of water vapor over the electrolyte / over pure water.	α_a, α_c	Charge transfer coefficient for anode/ cathode (both are 0.5 on the symmetry reactions).
a_i, v_i	Activity of species i and its coefficient.	j_a, j_c	The instantaneous current density passing through the anode/cathode.
$c_1^r, c_2^r, c_3^r, c_4^r$	Constant coefficients related to reversible voltage.	$j_{a,0}, j_{c,0}$	The another/cathode electrode exchange current density.
A	Cell surface.	$c_{k,log}^{act}, c_{k,j}^{act}, c_{k,ln}^{act}, c_{k,i}^{act}, k \in \{a, c\}$	Temperature-dependent coefficients related to the activation voltage.
l	The thickness of the cell.	$c_{k,j,0}^{act}, c_{k,j,-1}^{act}, c_{k,j,-2}^{act}, c_{k,ln,0}^{act}, c_{k,ln,1}^{act}, c_{k,ln,2}^{act}, c_{k,i,0}^{act}, c_{k,i,1}^{act}, c_{k,i,2}^{act}, k \in \{a, c\}$	Constant coefficients related to the activation voltage.
ρ	The specific electrical resistance of the cell.	$i_{act,a}, i_{act,c}$	The activation current that passes through anode /cathode.
$r_k^{ohm}, k \in \{1, 2, \dots, 8\}$	Constant coefficients related to ohmic voltage.	$\gamma_{act,a}, \gamma_{act,c}$	Pre-exponential factor for anode/cathode related to activation overvoltage.
R_{ohm}^{60}	The fitted resistance at 60°C.	$E_{act,a}, E_{act,c}$	Activation energy level for anode/cathode.
R_{ohm}^{stp}	Ohmic resistance at standard conditions.	$V^{act}(0), V^{con}(0)$	Initial value of activation/concentration overvoltage.
κ	Solution conductivity.	α_{app}	Apparent charge transfer coefficient.
κ_{60}	Solution conductivity at 60°C.	β	Exchange current density pre-factor.
d	Diaphragm thickness.		
M	Electrolyte molarity concentration.		
k_p, k_T	Curve fitting parameters related to pressure and temperature, respectively.		
$R_{ohm}^a/R_{ohm}^e/R_{ohm}^m/R_{ohm}^c/R_{ohm}^m$	The ohmic resistances of the anode/electrolyte/cathode/membrane.		
λ	The membrane humidification degree.		

β_a, β_c	The pre-factor for anodic/cathodic exchange current density.
$\Delta G_{act,a} / \Delta G_{act,c}$	Activation energies of the oxygen/hydrogen evolution.
ΔG_{act}	Average activation energy.
B	Tafel slope.
B_a / B_c	Tafel slope of anode/cathode.
r_1^{con} / r_2^{con}	Constant coefficients obtained from measurement tests.
$r_{w,1}^{con}, r_{w,2}^{con}$ $c_{w,1}^{con}, c_{w,2}^{con}$	Dimensionless Warburg coefficients related to resistance and capacitance of the concentration overvoltage.
$C_{O_2,m}, C_{H_2,m}$	Oxygen / hydrogen concentration at the membrane-electrode interface.
$C_{O_2,m}^0, C_{H_2,m}^0$	Oxygen/ hydrogen concentration at the membrane-electrode interface at standard conditions.
j	Current density of cell.
j_L	Limiting current density.
$P_{H_2}^k / P_{O_2}^k, k \in \{a, c\}$	Partial pressure of hydrogen/oxygen at anode/cathode.
$P_{H_2O}^k / P_{CO_2}^k / P_{CO}^k, k \in \{a, c\}$	Partial pressure of water/carbon dioxide/carbon monoxide at anode/cathode.
$D_{H_2O}^{eff}, D_{O_2}^{eff}$	The average effective diffusivity coefficient of water and oxygen.
ξ	The ratio of electrode tortuosity to porosity.
$D_{H_2O,H_2}, D_{H_2O,K}$	Ordinary molecular diffusion and Knudsen diffusion coefficient of water.
$H_a(s), H_b(s), H_c(s)$	Transfer functions of electrolysers in BD presentation.
P_e / P_e^{ref}	Real/reference electrical power consumption of electrolyser.
z, p_1, p_2	Zero and poles of electrolysers' transfer functions.
τ	Time constant of electrolysers' transfer functions.

I. INTRODUCTION

Efforts to encounter climate change have led to a shift from fossil fuels to renewable energy sources (RESs) like wind and solar in the energy sector. Various scenarios are being explored to generate electricity from RESs, aiming to reduce carbon emissions [1], [2], [3]. Additionally, there's a focus on incorporating clean fuels to mitigate greenhouse emissions from industries and transportation, especially in sectors that are difficult to electrify. Hydrogen is increasingly recognized as a key fuel for the future due to its versatility and broad applications. It is expected to play a vital role in achieving a clean and sustainable future, serving as a clean energy

carrier, long-term storage medium, and carbon-free fuel in transportation, aviation, manufacturing, and chemical industries [4], [5], [6].

Moreover, wind and solar power generation are subject to weather conditions, causing fluctuations in energy production and distribution. This variability can create imbalances between energy supply and demand, which highlights the importance of frequency regulation from the power system load section [7]. In this regard, energy storage technologies could be utilized to store surplus renewable energy during peak production periods for later usage during low generation times. One of the promising options to do so is integrating water electrolysis for hydrogen production using excess renewable energy, which helps mitigating the intermittent nature of renewables and lower green hydrogen production expenses [8].

Electrolysis stands out as one of the most effective techniques for producing hydrogen from water. Historically recognized as an electrochemical process, electrolysis involves the separation of water into hydrogen and oxygen [9]. Its origins trace back to the 1800s with the groundbreaking discovery of electric water splitting by Nicholson and Carlisle [10].

Electrolysis, particularly green electrolysis powered by renewable energy sources, has gained significant importance in recent years. Its scalability allows for a wide range of applications, from small-scale systems powered by a single wind turbine to large-scale installations integrated with the power grid. The hydrogen produced through electrolysis serves multiple purposes, including residential heating, energy storage, fueling stations, and industrial processes. Additionally, hydrogen can be utilized in fuel cells to regenerate electricity when needed. The various applications of hydrogen and its production path through electrolysers are illustrated schematically in Fig. 1, [11], [12].

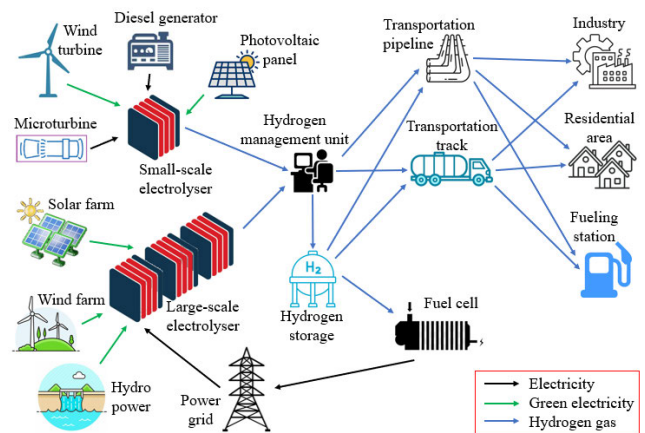


FIGURE 1. Application schematic of hydrogen derived from electrolysis.

Employing electrolysers alongside renewable electricity requires studying and analyzing not only their behavior but also their integration with RESs. Furthermore, ensuring the

efficient operation and control of renewable energy-based electrolysers and hydrogen storage systems mandates precise and thorough modeling of the system components, with particular emphasis on the electrical performance [8], [13].

The main types of electrolysers are Alkaline Electrolysers (AE), Proton Exchange Membrane Electrolysers (PEME), and Solid Oxide Electrolysers (SOE). AEs employ an alkaline electrolyte solution, like potassium hydroxide, and nickel electrodes, operating at lower temperatures with a long history of commercial applications. PEMEs utilize a solid polymer membrane, such as Nafion, to separate gases, operating at higher temperatures and pressures for improved efficiency and rapid response. SOEs rely on solid ceramic electrolytes like yttria-stabilized zirconia, functioning at high temperatures and capable of converting carbon dioxide and water vapor directly into syngas, showing promise for carbon capture applications [9], [14].

The electrical behavior of electrolysers can be studied using three main modeling formats: electrical equivalent circuit (EEC), mathematical formulation (MF), and block diagram (BD) presentation. An effective approach to analyzing electrolyser behavior is by utilizing a suitable EEC, which provides an electrical circuit representation for the electrolyser, facilitating its behavior modeling when it is supposed to be connected to other circuits in an electrical system. MF is another format for describing the electrical behavior of electrolysers, presenting their behavior through mathematical terms. Finally, the BD approach is well-suited for modeling electrolysers in dynamic studies, simplifying their control and operational analysis. The importance of dynamic studies is further emphasized in modern low-inertia power systems, where large loads like electrolysers are expected to play a critical role in providing frequency response and enhancing grid stability in future networks.

It is notable that provision of a suitable electrical model serves as a foundation for further electrolyser studies. In other words, proposing a proper electrical-based model for electrolysers establishes a solid base for further numerous studies and analyses in the field of electrical engineering. Among the pre-mentioned three types of modelling formats, EECs stand out as the simplest, most user-friendly, and direct approach for exploring electrolyser operation and control [8]. Therefore, this paper primarily examines papers that have introduced EEC models for electrolysers.

Several studies in the literature have examined electrolysers' behavior from an electrical perspective. Some have focused on modeling electrolysers' behavior via EEC or MF, while others have aimed to integrate and control electrolysers within power systems by BDs. Additionally, certain studies have investigated the dynamic behavior of electrolysers and their impact on the system's frequency response. In this context, the reviewed papers in this study have been gathered in Table 1 based on their objectives.

Many researchers have tried to study electrolysers from different points of view (which are represented in Table 1),

each addressing specific properties of these devices. Numerous papers have delved into the physics of electrolysers, analyzing their behavior through detailed mathematical models. While these works provide highly accurate representations, their complexity due to the intricate mathematics makes them more suitable for detailed studies focused on specific electrolyser designs. However, this complexity renders such models impractical for systematic studies, such as those required in power system simulations.

On the other hand, some studies have introduced EEC models to mitigate the excessive complexity of mathematical models. These EEC models offer a simplified approach, making them well-suited for electrical circuit simulation studies involving electrolysers. Nevertheless, most of the presented EEC models rely on specific experimental data, which limits their application to those conditions [8]. Similarly, BD models share this drawback, as they are often developed based on specific operating conditions of electrolysers. Moreover, relatively few studies have attempted to model electrolysers using this format. Despite this, BD models offer the advantage of simplicity, making them particularly useful for control studies of electrolysers.

A significant portion of the existing research focuses on AEs and PEMEs, which are relatively mature technologies with extensive studies addressing their performance, dynamics, and integration. In contrast, SOEs have received comparatively limited attention in the literature. As a result, research on SOEs is not as mature, leaving significant gaps in understanding their dynamics, operational challenges, and integration into broader energy systems.

In reference [14], an overview of electrolysis technologies for large-scale energy storage is provided, comparing their capacity, performance, flexibility, lifetime, and costs. However, this reference lacks reviewing any electrical equivalent circuit for electrolysers. Reference [5] reviews AE modeling with a focus on electrical domain and its specific electrolytic conductivity, but it does not consider all EECs related to AEs. References [8] and [15] study control methods and electrical equivalent circuits for PEMEs, respectively, without addressing other electrolyser types. Similarly, authors of [16] and [17] investigate specific physical phenomena related to SOEs. Notably, the reviewed papers mostly consider only one type of electrolyser, highlighting the need for a systematic review and categorization of electrical models for all electrolyser types.

In this regard, this paper overviews the electrical models proposed in the literature for all three electrolyser types (i.e., AE, PEME, and SOE). As mentioned previously, electrical models could be represented in EEC, MF, or BD formats. Hence, this paper, also, aims to classify electrical models from the EEC, MF, and BD perspectives. Additionally, a discussion as well as a comparison are done in this paper on the dynamic response of electrolysers, which is important especially in the transient behavior studies of electrolysers. All in all, the contributions

of this paper could be summarized in the following bullet points.

- Providing an overview on the electrical behavior of all three major electrolyser types (AE, PEME, and SOE).
- Classification of electrolyser models according to the proposed EEC schemes.
- Classification of electrolyser models based on MF.
- Classification of electrolyser models based on BD presentations.
- Discussion on the dynamic response of electrolysers.

The remaining sections of the paper are structured as follows. Section II provides a detailed exploration of electrolyser types and their operational principles. In Section III, existing studies on electrolyser modeling are categorized and classified. Section IV organizes references based on the suggested EEC models for electrolysers. Section V classifies reviewed papers according to their MF representations of electrolysers. In Section VI, BD models proposed for electrolysers are presented. Section VII discusses and compares the dynamic response of electrolysers, while section VIII delves into challenges related to electrolyser modeling. Finally, Section IX offers a conclusion to summarize the findings and contributions of the paper.

II. ELECTROLYSER TYPES AND THEIR OPERATIONAL PRINCIPLES

A vital component in transitioning to a hydrogen economy powered by RESs is the electrolyser, which facilitates converting clean electricity into hydrogen. In a standard electrolyser, water molecules undergo electrolysis, splitting into hydrogen and oxygen through the application of a direct electrical current across a cathode and anode immersed in an electrolyte (as shown in Fig. 2). Chemically, the dissociation reaction inside an electrolyser cell could be written as the following formula. The key elements of the electrolytic cell include electrodes, a diaphragm, and the electrolyte. The diaphragm permits the passage of ions while preventing the generated gases from passing through to avoid their mixture [17].

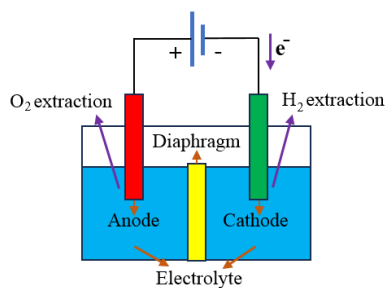
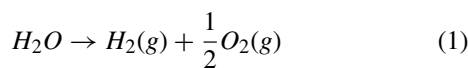


FIGURE 2. Electrolyser working principle and its structure [8], [9].

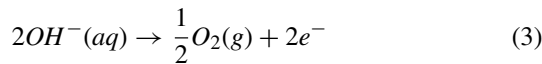
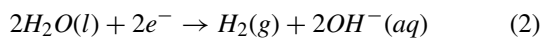
TABLE 1. Taxonomy of the reviewed papers based on their objectives.

Reference	Modelling electrolyser	Controlling electrolyser	Frequency dynamics study	Other objectives
[18], [19], [20], [21], [22], [23], [24], [25], [26]	✓	✓	✓	-
[27], [28], [29], [30], [31]	✓	✓	-	-
[6], [13], [32], [33], [34], [35], [36], [37]	✓	-	-	-
[38], [39]	-	✓	✓	-
[40]	✓	-	-	Analysis of the efficiency and specific energy consumption
[41]	✓	-	-	Studying the effect of diaphragm thickness, temperature and pressure on the performance of electrolyser
[14]	-	-	-	Review on the current status of electrolysers
[42], [43]	-	✓	-	Control strategy for efficiency/lifespan enhancement
[44]	-	✓	-	Review on control strategies for PEME
[15]	✓	✓	✓	Review on control aspects of hydrogen energy storage technologies
[5]	✓	-	-	Review on electrical domain and specific electrolytic conductivity of AEs
[45]	-	-	-	Designing an AE by minimizing the ohmic resistance
[8]	✓	-	-	Review on EECs of PEMEs
[17]	✓	-	-	Review on SOE modelling
[16]	✓	-	-	Review on the SOE modelling methods at various scale levels
[46]	✓	✓	-	Modeling a hybrid microgrid of fuel cell and photovoltaic and improving its efficiency
[47]	✓	✓	-	Inclusion of an electrolyser with a switching algorithm in a hybrid energy storage system
[48]	✓	✓	-	Proposing a system modeling and performance analysis of a renewable hydrogen energy hub connected to an AC/DC hybrid microgrid
[49]	✓	-	-	Optimizing a biomass-driven Rankine cycle that incorporates multi-effect desalination and a SOE to produce power, hydrogen, and freshwater.

A. ALKALINE ELECTROLYSER (AE)

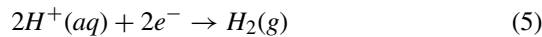
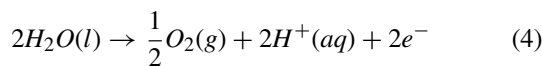
The preferred electrolyte for most applications is a 30% concentrated solution of potassium hydroxide, although sodium hydroxide and sodium chloride are also viable options. Diaphragms can be constructed from various materials such as ceramic oxides like asbestos and potassium titanate, as well as polymers like polypropylene and polyphenylene sulfide. Traditionally, asbestos diaphragms, typically 3 mm thick, have been common in conventional AE cells, but due to health concerns and limitations on operating temperature (not exceeding 80°C), alternatives have been being explored [50], [51].

The anode is typically made of steel with a nickel coating, while the cathode is made of steel with a catalyst coating, and there is usually a 5 mm gap between the two electrodes. In an AE cell, the following reactions (2) and (3) occur in the cathode and anode, respectively [52].



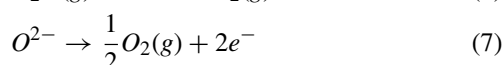
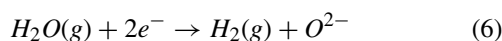
B. PROTON EXCHANGE MEMBRANE ELECTROLYSER (PEME)

In PEME cells, there exists a gas-tight, thin polymeric membrane with a cross-linked structure, typically less than 0.2 mm thick, possessing a distinctly acidic nature owing to the presence of sulfonic acid functional groups. These groups facilitate proton conduction within the material through an ion exchange mechanism. Nafion, a trademark of DuPont, is the most frequently utilized membrane for water electrolysis in PEME cells [52]. The reactions that take place in the anode and cathode of a PEME cell are demonstrated through reactions (4) and (5), respectively [53].



C. SOLID OXIDE ELECTROLYSER (SOE)

With the aim of reducing energy consumption and, consequently, operational expenses, SOE technology was created. The electrolyte of SOE consists of Yttria-stabilized zirconia (YSZ), which capitalizes on the oxygen vacancies within its mixed oxide structure, enabling superior ionic conductivity even under high operating temperatures. The anode is composed of a blend of YSZ and perovskites designed to enhance electrocatalysis by leveraging structural and electronic imperfections, while the cathode is a cermet made from nickel and YSZ [52]. Equations (6) and (7) indicate the reactions take place in the cathode and anode of a SOE cell, respectively [17].



D. COMPARISON OF ELECTROLYSER TYPES

Presently, AE and PEME technologies are commercially viable, whereas SOE technology is still in the developmental stage. AEs have a longer lifespan and lower overall cost compared to PEMEs. However, they suffer from low current density and operational pressure, leading to larger system volumes and higher hydrogen production costs [54]. On the other hand, PEMEs offer high cell efficiency and rapid system dynamics, making them appealing for integration into power grids, particularly grids with high share of RESs. Nevertheless, PEMEs are hindered by the high costs of platinum catalysts and lower lifespan [32]. SOE emerges as a promising technology for advancing sustainable development, enabling the recycling of CO₂ into usable fuels and contributing to the hydrogen economy. Additionally, SOEs exhibit superior efficiency compared to AEs and PEMEs due to their operation at high temperatures [14], [17].

A comprehensive comparison about advantages and disadvantages of different electrolyser types is presented in Table 2. Furthermore, Table 3 provides a detailed performance comparison of these electrolysers, highlighting their key attributes such as their lifespan and efficiency [9], [55], [56], [57], [58], [59]. Finally, Fig. 3. indicates a radar chart for a qualitative comparison of electrolyser types in a glance.

To enhance the efficiency, performance, and lifetime of electrolysers, various research papers have been conducted. For instance, the effects of varying temperatures and membrane thicknesses on the efficiency of PEM electrolysers under different pressures have been investigated in [60], while their performance under various inlet temperatures and current densities has been studied in [61]. Moreover, an innovative configuration of electrolysers, introduced in [62], incorporates efficient heat utilization through a mutual lye mixer, enabling faster hot-startup and enhanced performance by reducing heat loss and increasing startup speed. Additionally, [43] proposes a novel control strategy for multi-electrolyser systems. During the rapid start-up phase, this strategy optimizes performance by reducing the power of electrolysers operating at their rated capacity and redistributing this power to start additional electrolysers quickly. Finally, [63] presents a review of recent performance improvements in AE, focusing on advancements such as parametric optimization, overpotential reduction via innovative electrode materials, and novel separator designs.

One of the key metrics that demonstrates the performance of electrolysers is their efficiency. In general, the efficiency of electrolysers can be expressed using the following equation [40], [64]:

$$\eta_E = \eta_F \cdot \eta_V \cdot \eta_A \quad (8)$$

where, η_E is the electrolyser efficiency, and η_A demonstrates the efficiency of the auxiliary equipment (electrolyser water and heat management equipment). Moreover, η_V indicates the voltage efficiency responsible for the membrane loss as well as the heat loss. Finally, η_F , named faraday efficiency, refers to the gas diffusion losses.

TABLE 2. Pros and cons of each electrolyser type (pro = ✓, con = ✗).

AE	<ul style="list-style-type: none"> ✓ The most mature, widespread, and advanced electrolyser [54] ✓ Long lifetime [54] ✓ No need for a precious metal catalyst [50] ✓ Low global cost [54] ✓ Easy to manage due to the operation in moderate temperatures [53]
	<ul style="list-style-type: none"> ✗ Low current density [54] ✗ High system volume due to low operating pressure [54] ✗ High ohmic loss [50] ✗ Low efficiency [50]
PEME	<ul style="list-style-type: none"> ✓ High power and current density [54] ✓ Performance at high voltages [51] ✓ Low ohmic loss [51] ✓ High cell efficiency [32] ✓ Fast system dynamics [32] ✓ Wide partial load range and high operational adaptability [32] ✓ Permitting temporary overloading [51] ✓ High purity of generated gases [51] ✓ Safety owing to the unavailability of caustic electrolyte [51] ✓ Low possibility of flammable mixture generation due to small gaseous permeability [57] ✓ high pressurized hydrogen production [57] ✓ Capability of producing hydrogen and oxygen at a high rate [57] ✓ Small system volume [57] ✓ Low need for maintenance [5]
	<ul style="list-style-type: none"> ✗ High platinum catalysts costs [32] ✗ Significant initial investment [51] ✗ Short lifetime [32]
SOE	<ul style="list-style-type: none"> ✓ Allows CO₂ to be recycled into usable fuels [17] ✓ Ability to create syngas (by co-electrolyzing steam and CO₂) and ammonia (by co-electrolyzing with air) [9] ✓ Possibility of shaping in any desired specifications due to its solid components [17] ✓ High efficiency owing to high temperature operation [14] ✓ Possibility of reversible operation, operation as a fuel cell [9] ✓ Possibility of operation at thermoneutral cell voltage at much higher current densities once degradation is reduced [14] ✓ Not prone to leaks due to the solid electrolyte [9] ✓ Lower resistive loss owing to small design [9] ✓ Great potential to be deployed in large scale because of a high efficiency [16]
	<ul style="list-style-type: none"> ✗ Lower technology development compared to AE and PEME [17] ✗ Material stability challenge due to operation at high temperature [14] ✗ Its maintaining in idle mode is very energy consuming (Otherwise a long start-up time is necessary to heat the system up and to avoid the risk of thermal stress) [14] ✗ Greater capital costs due to the necessity for additional processing of the hydrogen-steam mix generated at the cathode [9] ✗ Challenges in degradation and short lifetime due to high steam concentration, high current densities and increased temperature [16] ✗ Not suitable for usage in the presence of fluctuating renewable energy owing to the impact of variations on thermal stability [14]

III. CLASSIFICATIONS OF STUDIES ON ELECTROLYSER MODELING

Research on electrolyser modeling in power grids can be categorized in various ways. This section adopts five perspectives to classify these works: the type of electrolyser studied, the

¹The efficiency derived using the Lower Heating Value (LHV) of hydrogen.

TABLE 3. Performance comparison of electrolysers.

Property	AE	PEME	SOE
Operating pressure (bar)	1-30	30-80	1
Operating temperature (°C)	60-80	50-80	650-1000
Typical current density (A/cm ²)	0.4-1.0	0.2-4.0	0.5-1.5
Development stage (deployed MW)	>1000	>100	<10
Electrical efficiency ¹ (%)	63-70	56-60	74-81
Degradation rate (% per 1000-hour)	0.13	0.25	0.55-1
Lifespan in full load (10000 hours)	6-10	5-9	2-5

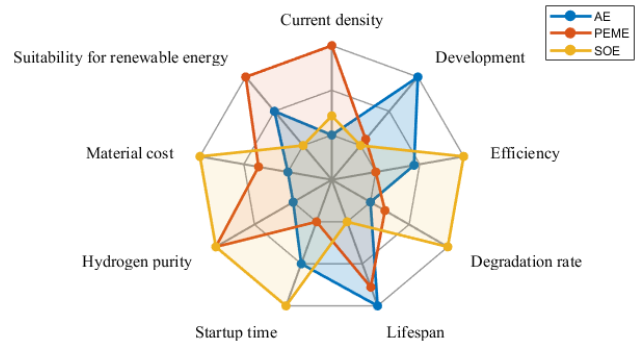


FIGURE 3. Qualitative comparison of electrolysers.

scope of the study (static or dynamic behavior), the modeling approach employed, the level of modeling (cell or stack), and the consideration of power-electronic interface (to be able to be connected to the power grid). These categories are visually represented in Fig. 4. for clarity.

Electrolysers are mainly classified as AE, PEME, or SOE, according to their types. Also, studies may focus on either the static or dynamic behavior of electrolysers, leading to their categorization as static or dynamic. Furthermore, modeling approaches vary, including physical/phenomenological (white-box), empirical (black-box), and semi-empirical (grey-box) modeling [65]. Empirical modeling, which has advanced alongside computational capabilities, does not require a deep understanding of the underlying physics and relies heavily on experimental data for calibration. In contrast, physical /phenomenological models are grounded in physical laws and offer insight into the behavior of the system. Parameters in such models hold physical significance, distinguishing them from empirical or semi-empirical models [17]. Additionally, studies on electrolysers can focus either on a single cell model or on an electrolyser stack. An electrolyser cell is an individual unit that performs the electrolysis of water, whereas an electrolyser stack consists of multiple cells connected in series or parallel. This configuration enables higher hydrogen production by increasing the overall capacity of the system [66].

Papers that aim to model electrolysers behavior have been also classified in more detail according to the five prementioned characteristics in Table 3.

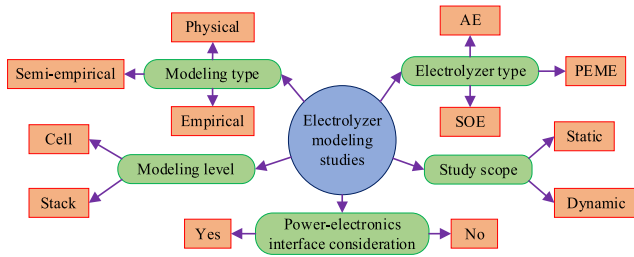


FIGURE 4. Considered categories for electrolyzer modeling studies.

TABLE 4. Taxonomy of electrolyzer modeling studies based on the defined categories.

Reference	Electrolyzer type	Study scope (S=static, D=dynamic)	Modeling level (C=cell, S=stack)	Modeling type (E=Empirical, SE=semi-empirical, P=physical)	Power-electronics interface consideration
[18], [20]	AE/PEME	D	S	E	✓
[26]	AE/PEME	D	C/S	E	✓
[19], [21]	PEME	D	S	E	✓
[13]	AE	S/D	C/S	P	-
[40]	PEME	S/D	C/S	E/SE	-
[41]	AE	S	C	SE	-
[15]	AE/PEME	D	C	E	✓
[6]	AE/PEME	S	S	E	-
[5]	AE	S/D	C/S	E/SE/P	-
[27]	AE	S/D	C	P	✓
[23], [28], [32]	PEME	D	S	E	-
[33]	PEME	D	C	E/P	✓
[22]	AE	D	C/S	E	✓
[8]	PEME	S/D	C/S	E/SE/P	-
[17]	SOE	S	C	E/P	-
[34]	SOE	S	C/S	P	-
[24]	AE/PEME	S/D	C/S	E	✓
[25]	PEME	D	C/S	E	✓
[29]	AE	D	C/S	SE	-
[30]	AE	D	C/S	SE	✓
[31]	SOE	D	S	P	-
[46], [47]	PEME	S	C	P	✓
[48]	PEME	S	C	E	✓
[16], [35], [49]	SOE	D	C/S	P	-
[36], [37]	PEME	S	C	E	-

IV. EEC PRESENTATION OF ELECTROLYSERS

Electrical Equivalent Circuit (EEC) models utilize electrical components such as voltage/current sources, resistors, inductors, and capacitors to replicate the behavior of various devices or systems. In the case of electrolysers, efforts are focused on creating an electrical representation that accurately mimics the voltage variations experienced during operation. These EEC estimations are often derived from

experimental polarization curves, which serve as the basis for developing empirical equations. Additionally, some models aim to capture the physical phenomena occurring within electrolysers. This section offers a thorough classification and categorization of the latest EEC models found in electrolyser literature. Typically, an electrolyser cell voltage is represented by the following general equation [13], [14], [17].

$$V_{cell} = V_{rev} + V_{ohm} + V_{act} + V_{con} \tag{9}$$

As equation (9) indicates, within electrolysers, four elements contribute to overvoltage from an electrical point of view. These elements encompass reversible voltage, ohmic voltage drop, activation overvoltage, and concentration overvoltage. overvoltage, also known as overpotential, is the additional voltage that needs to be applied to an electrode in an electrochemical cell beyond the thermodynamically required voltage to drive a reaction at a desired rate. Further elucidation on the aforementioned overvoltage components is provided in the next section.

Also, using equation (9), a general EEC model can be created, as illustrated in Fig. 5, to represent an overview of EECs given for electrolysers in the literature. Each voltage component in this circuit model can be simulated using a combination of electrical circuit components, resulting in a precise or approximate model for actual phenomena associated with the voltage drop. In this domain, researchers have suggested various EECs to model the electrical behavior of electrolysers. This section compiles all the proposed EECs from the reviewed literature and classifies them within Table 5, along with the corresponding electrolyser types. It is important to note that, based on the literature review, no EEC model has been proposed for SOEs yet.

Furthermore, it is notable that some EECs incorporate the consideration of the Double Layer Effect (DLE) within the electrolyser instead of activation and concentration overvoltage. Double layer effect refers to the phenomenon that occurs when charge accumulates on both sides of the membrane, accompanied by an opposite charge on the electrodes' surfaces, leading to capacitive effects at the anode and cathode sides of the membrane. In EEC models, this phenomenon can be replicated by incorporating a parallel combination of a capacitor and a resistor component on both the anode and cathode sides. The voltage drop attributed to the double-layer effect in the electrolyser is a composite of the activation and concentration overvoltage components. Hence, some studies integrate the activation and concentration overvoltage components using the concept of the double layer effect [67].

V. MF PRESENTATION OF ELECTROLYSERS

Mathematical formulation (MF) modeling is essential for comprehending and analyzing the electrical behavior of electrolysers. As outlined in the preceding section, the terminal voltage of electrolysers is influenced by four distinct overvoltages corresponding to specific physical phenomena. These phenomena—reversible voltage, ohmic voltage drop, activation overvoltage, and concentration overvoltage—are

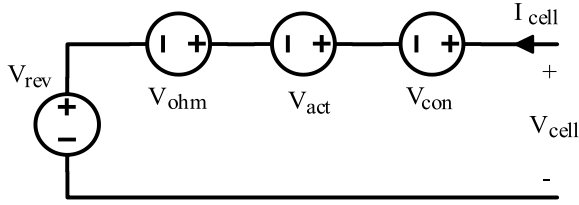


FIGURE 5. General EEC model of an electrolyser cell [8], [17], [18].

detailed in the subsequent subsections, providing a comprehensive exploration of the mathematical frameworks employed to study their electrical behavior.

A. REVERSIBLE VOLTAGE

The reversible potential, also known as the open circuit voltage, denotes the minimum voltage necessary to initiate electrolysis [13], [17]. It also represents the voltage consumed by the reversible reaction, thereby facilitating hydrogen production. This voltage typically varies with changes in operating temperature and pressure; however, some studies treat it as a constant in EEC models, often emulating it with a constant DC voltage battery component [8]. Table 6 outlines the equations proposed for modeling the reversible voltage of electrolysers. It is worth noting that in the equations presented in Table 6, the variable n signifies the number of moles of electrons exchanged to produce a mole of hydrogen in the electrolyser. For all electrolyser types, including AE, PEME, and SOE, the value of n remains constant at two, as evidenced by equations (2), (5), and (6).

B. OHMIC VOLTAGE DROP

Ohmic overvoltage signifies the energy consumed as electric charge carriers encounter resistive barriers within the electrolysis cell. This resistance arises from various sources, including electrolyte resistance, membrane ohmic resistance, and electrode resistances at both the anode and cathode. Different models proposed in the literature adopt varying approaches to account for these resistive components, with some incorporating all elements for a precise representation of the ohmic voltage drop, while others offer some approximations. Nevertheless, across the literature surveyed, the ohmic voltage drop is commonly represented by a series resistor to encapsulate the electrical resistance hindering current flow. Consequently, the voltage drop resulting from this resistance can be formulated as follows [13], [33], [35].

$$V^{ohm} = R^{ohm} I_{cell} \tag{10}$$

Various proposed formulae in the literature for obtaining the ohmic resistor are represented in Table 7.

C. ACTIVATION OVERVOLTAGE

From an electrical standpoint, activation overvoltage serves to simulate two primary phenomena. Firstly, it represents

TABLE 5. Proposed electrolyser EECs in the literature.

EEC No	Electrolyser type	EEC schematic	References
1	AE		[15], [18], [20]
2	PEME		[18], [19], [20], [21]
3	AE		[5], [13], [26]
4	AE/PEME		[8], [15], [24], [28], [32], [40]
5	AE		[5]
6	PEME		[8], [26], [33]
7	PEME		[33]
8	PEME		[8], [36], [37], [46], [47], [48]
9	PEME		[8]
10	PEME		[8]

TABLE 5. (Continued.) Proposed electrolyser EECs in the literature.

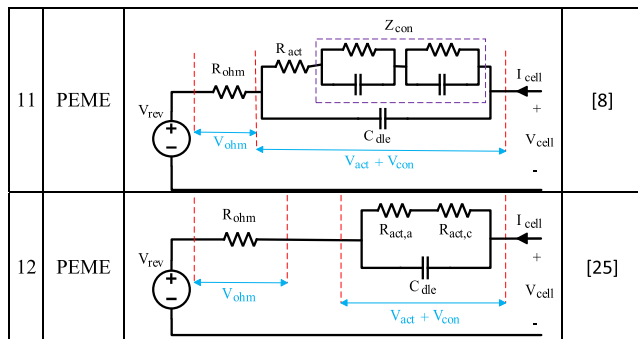


TABLE 6. Proposed formulations for the reversible voltage of electrolysers.

Reversible voltage formulation	ref
Constant reversible voltage	[20], [24], [26], [28], [29], [32], [36], [37], [45], [46], [47]
$V_{rev} = -\frac{\Delta G}{nF}$	[14], [15], [17], [30], [31], [33], [34], [36], [37], [40]
$V_{rev} = V_{rev}^{stp} + \frac{RT}{nF} \ln\left(\frac{P}{P^{stp}}\right)$	[8], [18], [19], [21], [37], [48]
$V_{rev} = V_{rev}^{stp} + \frac{RT}{nF} \ln\left(\frac{P_{H_2} \sqrt{P_{O_2}}}{P_{H_2O}}\right)$	[8], [25], [31], [34], [35], [49]
$V_{rev} = V_{rev}^{stp} + \frac{RT}{nF} \ln\left(\frac{(P - P_{H_2O})^{1.5}}{(P_{H_2O}/P_{H_2O}^0)}\right)$	[5], [13], [27], [41]
$V_{rev} = V_{rev}^{stp} + \frac{RT}{nF} \ln\left(\frac{\prod_{i \in products} a_i^{v_i}}{\prod_{i \in reactants} a_i^{v_i}}\right)$	[16]
$V_{rev} = c_1' - c_2'T + c_3'T \ln T + c_4'T^2$	[22]

the resistance encountered in freeing electrons from charged electrode surfaces, known as charge transfer resistance. Secondly, it reflects the time delay incurred by accumulated charge on both sides of the membrane at the anode and cathode, which fluctuates with changes in electrolyser current [17], [18]. Consequently, as outlined in Table 5, papers typically propose a combination of a resistor element to mimic the heat energy required for electron release from electrode surfaces and a capacitor element to replicate the charge accumulation as well as time delay associated with current variations. Table 8 provides a comprehensive overview of the formulae proposed in the literature for modeling the activation overvoltage.

TABLE 7. Proposed formulations for the ohmic resistance of electrolysers.

Ohmic resistance formulation	ref
Constant ohmic resistance	[8], [14], [15], [16], [17], [18], [20], [21], [24], [26], [28], [32], [36], [37], [46], [47]
$R_{ohm} = \frac{\rho l}{A}$	[25], [33], [45]
$R_{ohm} = \frac{1}{A} (r_1^{ohm} + r_2^{ohm} T)$	[5], [30]
$R_{ohm} = \frac{1}{A} \left(r_1^{ohm} + r_2^{ohm} T + \frac{r_3^{ohm}}{T} + \frac{r_4^{ohm}}{T^2} \right)$	[13]
$R_{ohm} = \frac{1}{A} (r_1^{ohm} + r_2^{ohm} T + r_5^{ohm} P)$	[5], [29]
$R_{ohm} = \frac{1}{A} \left(r_1^{ohm} + r_2^{ohm} T + r_6^{ohm} M \right) + \frac{1}{A} \left(r_7^{ohm} M^2 + r_8^{ohm} d \right)$	[5]
$R_{ohm} = R_{60}^{ohm} \frac{\kappa}{\kappa_{60}} (0.26 + 1.48d)$ $\kappa = -2.04M - 2.8 \times 10^{-3} M^2 + 5.33 \times 10^{-3} MT$ $+ 207 \frac{M}{T} + 1.04 \times 10^{-3} M^3 - 3 \times 10^{-7} M^2 T^2$	[41]
$R_{ohm} = R_{stp}^{ohm} + k_p \ln\left(\frac{P}{P^{stp}}\right) + k_T (T - T_{stp})$	[19], [37], [48]
$R_{ohm} = \frac{(\rho_a l_a + \rho_c l_c)}{A} + \frac{l_m}{\sigma_m}$ $\sigma_m = (0.005139\lambda - 0.00326) e^{1268\left(\frac{1}{303} - \frac{1}{T}\right)}$ $\lambda = 0.08533T - 6.77632$	[40]
$R_{ohm} = R_a^{ohm} + R_e^{ohm} + R_c^{ohm} = \rho_a l_a + \rho_e l_e + \rho_c l_c$	[34], [35]
$R_{ohm} = R_a^{ohm} + R_e^{ohm} + R_c^{ohm} = \frac{l_a}{\sigma_a} + \frac{l_e}{\sigma_e} + \frac{l_c}{\sigma_c}$ $\sigma_e = 33400 e^{-\frac{10300}{T}}$	[31]
$R_{ohm} = R_a^{ohm} + R_e^{ohm} + R_c^{ohm} = \sum_{i \in \{a,e,c\}} r_i^{ohm} l_i e^{\frac{r_i^{ohm}}{T}}$	[49]

D. CONCENTRATION OR DIFFUSION OVERVOLTAGE

In several sources, EECs often stem from empirical equations derived from polarization curves based on actual experimental data. Consequently, the impacts of activation and concentration overvoltage are frequently intertwined and associated with the double-layer capacitance effect. Essentially, when deduced from the polarization curve, these impacts cannot be distinctly isolated, as they both contribute to the double-layer capacitance effect [8], [17]. Nonetheless, certain papers have endeavored to separate these overvoltages

TABLE 7. (Continued.) Proposed formulations for the ohmic resistance of electrolysers.

$R_{ohm} = R_a^{ohm} + R_e^{ohm} + R_c^{ohm} + R_m^{ohm},$ $R_a^{ohm} + R_c^{ohm} = \frac{1}{A} \left(\frac{l_a}{\sigma_a} + \frac{l_c}{\sigma_c} \right),$ $\sigma_a = \sigma_c = 6000000 - 279650T + 532T^2 - 0.38057T^3,$ $R_{ohm}^e = R_{ohm}^{e,bf} + R_{ohm}^{e,b},$ $R_{ohm}^{e,bf} = \frac{l_{a,m} + l_{c,m}}{\sigma_{e,bf} A},$ $\sigma_{e,bf} = -204.1M - 0.28M^2 + 0.5332MT + 20720 \frac{M}{T} + 0.1043M^3 - 0.00003M^2T^2,$ $R_{ohm}^{e,b} = R_{ohm}^{e,bf} \left(\left(\frac{A}{A_{eff}} \right)^{1.5} - 1 \right),$ $R_{ohm}^m = \frac{0.06 + 80e^{50}}{10000A}$	[5], [27]
--	-----------

and put forth specific formulas for modeling them. The concentration overvoltage—which results from the limitations on mass transferrin the porous electrodes—are described in the MF outlined in Table 9.

VI. BD REPRESENTATION OF ELECTROLYSERS

Aside from EECs, electrolysers could also be represented using BDs, which are particularly valuable for control-related studies. Numerous researchers have endeavored to capture electrolyser behaviors by devising BDs. Within the literature, three distinct transfer functions—as in equations (11) to (13)—have been suggested for this purpose. Where, *k* is the ratio of the electrolyser’s rated capacity to the total capacity of the power system [22].

In this context, the transfer function (11) is derived from experimental results in [68], where ramp-up and ramp-down tests were conducted for AE and PEME. These tests involved a 40 kW AE unit manufactured by Teledyne Technologies and a 40 kW PEME unit produced by Proton OnSite. The DC load set-points of both electrolysers were rapidly varied to assess their ramping capabilities. Based on these experiments, Dozein et al. proposed the transfer function (11) to capture the observed dynamic behavior. Since this model is directly derived from experimental results, it provides the most accurate BD model for these electrolysers.

However, while (11) is a precise model, it cannot be used to develop an EEC due to the order difference of its denominator and numerator which is equal to two [69]. To address this limitation, an approximate transfer function, equation (12), was developed to enable EEC modeling, resulting in EEC model 1, as shown in Table 5.

TABLE 8. Proposed formulations for the activation overvoltage of electrolysers.

Activation phenomenon formulation	Ref
Constant activation resistance (R_{act})	[8]
Fixed-value parallel RC circuit Or $V_{act} = R_{act} \cdot L^{-1} \left[\frac{1}{R_{act} C_{act} s + 1} \int_0^\infty I_{cell}(t) e^{-st} dt \right] + V_{act}(0) e^{\frac{-t}{R_{act} C_{act}}}$	[8], [18], [19], [20], [21], [24], [25], [28], [32]
$V_{act} = V_{act,a} + V_{act,c}$ $V_{act,a} = \frac{RT}{\alpha_a nF} \log \left(\frac{j_a}{j_{a,0}} \right)$ $V_{act,c} = \frac{RT}{\alpha_c nF} \log \left(\frac{j_c}{j_{c,0}} \right)$	[5], [15], [25], [27], [40]
$j_{a,0} = 30.4 - 0.206T + 0.00035T^2$ $j_{c,0} = 13.72491 - 0.09055T + 0.09055T^2$ $\alpha_a = 0.0675 + 0.00095T$ $\alpha_c = 0.1175 + 0.00095T$	[5], [27]
$V_{act} = V_{act,a} + V_{act,c}$ $V_{act,a} = c_{a,\log}^{act} \log \left(c_{a,j}^{act} j_a + 1 \right),$ $c_{a,j}^{act} = c_{a,j,0}^{act} + c_{a,j,-1}^{act} T^{-1} + c_{a,j,-2}^{act} T^{-2}$ $V_{act,c} = c_{c,\log}^{act} \log \left(c_{c,j}^{act} j_c + 1 \right),$ $c_{c,j}^{act} = c_{c,j,0}^{act} + c_{c,j,-1}^{act} T^{-1} + c_{c,j,-2}^{act} T^{-2}$	[5], [29], [30]
$V_{act} = V_{act,a} + V_{act,c}$ $V_{act,a} = c_{a,\ln}^{act} \ln \left(\frac{1}{c_{a,i}^{act}} i_{act,a} + 1 \right),$ $c_{a,\ln}^{act} = c_{a,\ln,0}^{act} + c_{a,\ln,1}^{act} T + c_{a,\ln,2}^{act} T^2,$ $c_{a,i}^{act} = c_{a,i,0}^{act} + c_{a,i,1}^{act} T + c_{a,i,2}^{act} T^2$ $V_{act,c} = c_{c,\ln}^{act} \ln \left(\frac{1}{c_{c,i}^{act}} i_{act,c} + 1 \right),$ $c_{c,\ln}^{act} = c_{c,\ln,0}^{act} + c_{c,\ln,1}^{act} T + c_{c,\ln,2}^{act} T^2,$ $c_{c,i}^{act} = c_{c,i,0}^{act} + c_{c,i,1}^{act} T + c_{c,i,2}^{act} T^2$	[13], [26]
$V_{act} = \frac{RT}{\alpha_a nF} \sinh^{-1} \left(\frac{j_a}{2j_{a,0}} \right) + \frac{RT}{\alpha_c nF} \sinh^{-1} \left(\frac{j_c}{2j_{c,0}} \right)$	[16], [31], [33]
$V_{act} = \frac{RT}{nF} \sinh^{-1} \left(\frac{j_a}{2j_{a,0}} \right) + \frac{RT}{nF} \sinh^{-1} \left(\frac{j_c}{2j_{c,0}} \right),$ $j_{0,i} = \gamma_{act,k} e^{\frac{E_{act,k}}{RT}}, k \in \{a, c\}$	[17], [34], [35], [49]

TABLE 8. (Continued.) Proposed formulations for the activation overvoltage of electrolysers.

$V_{act} = \frac{RT}{nF} \left(\frac{j_a}{j_{0,a}} + \frac{j_c}{j_{0,c}} \right)$ $j_{0,i} = \gamma_{act,k} e^{-\frac{E_{act,k}}{RT}}, k \in \{a, c\}$	[17]
$V_{act} = -1.476 e^{-\frac{5}{0.02} I_{cell}}$	[8], [36], [37], [48]
$V_{act} = \frac{2RT \ln 10}{\alpha_{app} F} \left(\log \frac{I_{cell}}{\beta A} + \frac{\Delta G_{act}}{RT \ln 10} \right)$ $\alpha_{app} = \frac{2\alpha_a \alpha_c}{\alpha_a + \alpha_c}$ $\Delta G_{act} = \frac{B_a \Delta G_{act,a} + B_c \Delta G_{act,c}}{B}$ $B = B_a + B_c$ $\beta = \beta_a^B \cdot \beta_c^B$	[41]

In some studies, for simplicity, the dynamic behavior of electrolysers is approximated by a time-delayed load model, as also discussed in [7]. With this approach, each electrolyser is modeled with a single time constant, as in equation (13), making it easier to work with in large-scale simulations where detailed dynamic behavior is not necessary.

It is noteworthy that these BD presentations are proposed only for AEs as well as PEMEs, and there are no transfer functions for SOEs in the reviewed literature. A brief overview of the BD models that have been suggested for electrolysers in the literature are also provided within Table 10.

$$H_a(s) = \frac{P_e}{P_e^{ref}} = k \frac{p_1 p_2}{(s - p_1)(s - p_2)} \quad (11)$$

$$H_b(s) = \frac{P_e}{P_e^{ref}} = k \frac{-p_1 p_2}{z} \cdot \frac{(s - z)}{s^2 - (p_1 + p_2)s + p_1 p_2} \quad (12)$$

$$H_c(s) = \frac{P_e}{P_e^{ref}} = k \frac{1}{\tau s + 1} \quad (13)$$

VII. DYNAMIC RESPONSE ASSESSMENT

Since the thermal system of an electrolyser has a time constant in the range of hours, it's reasonable to overlook thermal dynamics by presuming the electrolysis stack temperature remains constant during electrical dynamic studies. Because the internal stack temperature remains steady throughout the simulation period crucial to frequency response analysis, the internal pressure within the stack could similarly be presumed constant [18]. Additionally, since there's no feedback signal from the hydrogen production system to either the electrical or thermal components, the dynamics of hydrogen production will not impact electrical dynamics [19]. Consequently, it's deduced that the internal stack temperature and pressure exert

TABLE 9. Proposed formulations for the concentration overvoltage of electrolysers.

Concentration phenomenon formulation	Ref
Constant concentration resistance R_{con}	[8]
Fixed-value parallel RC circuit Or $V_{con} = R_{con} L^{-1} \left[\frac{1}{R_{con} C_{con} s + 1} \int_0^\infty I_{cell}(t) e^{-st} dt \right]$ $+ V_{con}(0) e^{-\frac{t}{R_{con} C_{con}}}$	[8], [19], [24]
$R^{con} = r_1^{con} \ln \left(\frac{r_2^{con}}{A} I_{cell} + 1 \right)$	[18], [20], [21]
Two parallel RC branches in series Or Warburg impedance $Z_{con}(s) = R_{con} \left(\frac{\tanh \sqrt{R_{con} C_{con} s}}{\sqrt{R_{con} C_{con} s}} \right) \approx$ $R_{con} \left(\frac{r_{w,1}^{con}}{r_{w,1}^{con} C_{w,1}^{con} R_{con} C_{con} s + 1} + \frac{r_{w,2}^{con}}{r_{w,2}^{con} C_{w,2}^{con} R_{con} C_{con} s + 1} \right)$	[8]
$V_{con} = \frac{RT}{nF} \ln \left(1 - \frac{j}{j_L} \right)$	[17]
$V_{con} = V_{con,a} + V_{con,c}$ $V_{con,a} = \frac{RT}{nF} \ln \left(\frac{C_{O_2,m}}{C_{O_2,m}^0} \right)$ $V_{con,c} = \frac{RT}{nF} \ln \left(\frac{C_{H_2,m}}{C_{H_2,m}^0} \right)$	[40]
$V_{con} = V_{con,a} + V_{con,c}$ $V_{con,a} = \frac{RT}{nF} \ln \left(\frac{P_{H_2}^a \sqrt{P_{O_2}^a}}{P_{H_2O}^a} \right) = \frac{RT}{nF} \ln \left(\frac{P_{CO}^a \sqrt{P_{O_2}^a}}{P_{CO_2}^a} \right)$ $V_{con,c} = \frac{RT}{nF} \ln \left(\frac{P_{H_2}^c \sqrt{P_{O_2}^c}}{P_{H_2O}^c} \right) = \frac{RT}{nF} \ln \left(\frac{P_{CO}^c \sqrt{P_{O_2}^c}}{P_{CO_2}^c} \right)$	[17]
$V_{con} = V_{con,a} + V_{con,c}$ $V_{con,c} = \frac{RT}{nF} \ln \left(\frac{1 + \frac{RT \cdot j l_c}{2FD_{H_2O}^{eff} P_{H_2}}}{1 - \frac{RT \cdot j l_c}{2FD_{H_2O}^{eff} P_{H_2O}}} \right)$ $V_{con,a} = \frac{RT}{2nF} \ln \left(1 + \frac{RT \cdot j l_a}{4FD_{O_2}^{eff} P_{O_2}} \right)$ $\frac{1}{D_{H_2O}^{eff}} = \xi \left(\frac{1}{D_{H_2O,H_2}} + \frac{1}{D_{H_2O,K}} \right)$	[31], [34], [49]

minimal effects on stack dynamics and can be treated as constant in dynamic analyses [18], [19], [33].

TABLE 10. Proposed BD models for electrolysers in the literature.

BD presentation	References
$P_e^{ref} \rightarrow H_a(s) \rightarrow P_e$	[18], [20]
$P_e^{ref} \rightarrow H_b(s) \rightarrow P_e$	[15], [18], [20], [21]
$P_e^{ref} \rightarrow H_c(s) \rightarrow P_e$	[22], [23], [68]

In dynamic studies of electrolysers, particularly focusing on AEs and PEMEs, operating at nominal temperatures enables them to adjust their full load range within a time frame of less than one second to a few seconds [14]. This flexibility enables both AE and PEME to provide grid balancing service effectively. Frequency-regulation experiments conducted at NREL showed similar performance between AEs and PEMEs, indicating both technologies can add or remove stack power to offer a sub-second response that mitigates duration of frequency disturbances in microgrids. Hydrogenics, offering AE and PEME technologies, affirms both technologies can react rapidly (with a response delay less than one second) to stabilize power grids when running and at operating temperature [14]. However, experimental results from [18], [69] suggest the time delay in AE response is greater than in PEMEs. Consequently, PEMEs exhibit faster dynamics than AEs, rendering them more suitable for virtual inertia and primary frequency response applications [15], [18], [20]. This discrepancy in response speed arises from the DLE phenomenon within electrolysers, where the capacitance component is notably larger in AEs compared to PEMEs. DLE phenomenon is due to non-uniform distribution of charges at the electrode-electrolyte interface, creating an energy barrier layer against electron flow during sudden current changes, thereby causing a response delay [19]. According to the case studies in [18], the ratio of DLE capacitance value in AE (C_{dle}^{AE}) to PEME (C_{dle}^{PEME}) could be obtained as follows:

$$\frac{C_{dle}^{AE}}{C_{dle}^{PEME}} = \frac{14\mu F}{1.93\mu F} \simeq 7.25 \quad (14)$$

Also, according to the data given in [18] and [20], which is based on experiments in [69], AE and PEME responses to a step signal are depicted in Fig. 6. Notably, the AE response, unlike PEME, exhibits a delay, and the ratio of rise times and settling times in AE to PEME (i.e., $\frac{t_{rise}^{AE}}{t_{rise}^{PEME}}$ and $\frac{t_{sett}^{AE}}{t_{sett}^{PEME}}$) can be calculated as follows:

$$\frac{t_{rise}^{AE}}{t_{rise}^{PEME}} = \frac{1s}{20ms} = 50, \quad \frac{t_{sett}^{AE}}{t_{sett}^{PEME}} = \frac{4s}{60ms} \simeq 66.7 \quad (15)$$

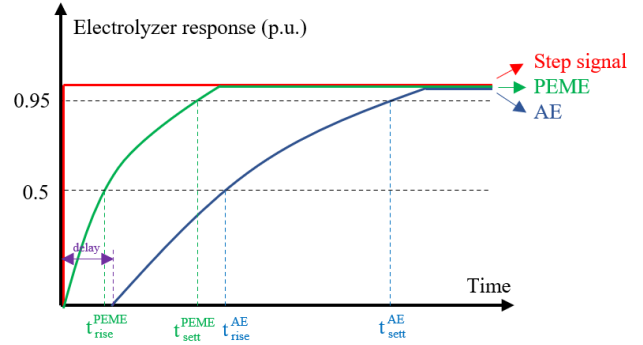


FIGURE 6. Dynamic response of AE and PEME to a step signal [18], [20].

VIII. CHALLENGES IN ELECTROLYSER MODELING

Given the vast applications and growing interest in green hydrogen, electrolyser plants are expected to play a significant role in power systems. However, several challenges and limitations associated with electrolyser plants must be addressed to ensure their effective integration and operation.

In this regard, the electrolysers that are powered by RESs are affected by their intermittent nature, which compromises operation and efficiency. This results in the degradation of internal components like current collectors and catalyst plates, reducing both hydrogen production productivity and purity and shortening the device’s lifespan. To address the growing demand for hydrogen, reliable electrolyser operation necessitates advanced power electronics controls and energy coordination strategies to counteract the irregularity of resources on the grid. Additionally, advancements in material science can improve electrolyser performance by introducing cost-effective materials with higher resistance to deterioration for manufacturing internal electrolyser plates [70], [71].

High-pressure operation in electrolysers can cause gas permeation through the membrane, posing risks such as hydrogen migration and potential explosions. While increasing membrane thickness can limit hydrogen passage, it also raises membrane ohmic resistance, reducing efficiency. To mitigate issues like bubble formation, gas permeation, and water starvation due to high-pressure conditions, techniques for removing produced gases and enhancing membrane materials are necessary [8].

The literature provides a wealth of mathematical formulations that model the detailed behavior of electrolysers. Numerous studies have extensively analyzed the chemical behavior of all three primary types of electrolysers, offering deep insights into their operational characteristics and underlying mechanisms. In other words, despite the EEC and BD modeling, the body of research on electrolysers is rich in MF modeling.

For EEC modeling, numerous studies have aimed to develop and propose EEC models within the electrical engineering domain. However, their applicability is limited

to specific electrolyser devices and operating conditions, restricting their generalization.

From the perspective of BD modeling, in electrical dynamic studies, electrolysers are often characterized by a response delay, typically represented by time-delay models. Nonetheless, similar to EEC models, BD models are also derived from specific devices operating under particular conditions. As a result, the parameters of these models are tied to the specific operating environment of the associated electrolyser, making them unsuitable for application across all operating conditions.

Consequently, improved modeling and parameter estimation techniques are needed to develop comprehensive and generalized models for studying electrolysers' performance.

Another significant challenge in the realm of electrolysers is associated with SOEs. SOECs degrade due to secondary and mechanical stress from operating at high temperatures, leading to higher capital costs due to the additional processing required for the hydrogen-steam mix produced at the cathode. They are unsuitable for use with fluctuating RESs due to the effect of load variations on thermal stability [9]. Moreover, Unlike AEs and PEMEs, SOEs have not been extensively researched, and there is a lack of EEC and BD models for them in the literature. Additionally, there is a need for more studies, particularly focusing on the dynamics and frequency response of SOEs in power systems.

The widespread adoption of electrolysers holds significant promise, but several challenges remain for large-scale grid deployment. One major barrier is their high capital cost, which, although reduced in recent years, remains substantial. These costs are associated not only with the electrolyser units themselves but also with the supporting infrastructure, including storage and distribution systems. In addition, the seamless integration of large-scale electrolysers into the power grid requires the development of advanced control strategies and effective coordination with other grid elements to ensure stable and efficient operation [72].

Another critical challenge is the low round-trip efficiency of hydrogen. Hydrogen must be compressed, transported, and stored before being converted back into energy through fuel cells. Each of these steps involves energy losses, limiting the overall round-trip efficiency to a maximum of approximately 40% [73]. Hence, to enable the large-scale deployment of electrolysers within power grids, further research and development are essential to address these technical and economic challenges and improve electrolyser performance.

IX. CONCLUSION

In conclusion, this paper has provided a comprehensive overview of the electrical behavior of the three major electrolyser types: AE, PEME, and SOE. Through an examination of existing literature, the paper has classified electrolyser models according to their proposed EEC schemes, MF presentations, and BD representations. Additionally, the paper has discussed the dynamic response of electrolysers, emphasizing its importance in transient behavior studies. By addressing

these topics, the paper has contributed to the understanding of electrolyser behavior and modeling techniques. However, challenges remain in electrolyser modeling, particularly in accurately representing their electrical behavior across different devices and operating conditions. Future research efforts should prioritize addressing these challenges, with particular emphasis on SOEs, which have received less attention, to develop more comprehensive and precise models for electrolyser systems.

REFERENCES

- [1] M. Tofighi-Milani, S. Fattaheian-Dehkordi, and M. Fotuhi-Firuzabad, "A new peer-to-peer energy trading model in an isolated multi-agent microgrid," *J. Appl. Res. Electr. Eng.*, vol. 1, no. 1, pp. 33–41, Jun. 2022.
- [2] M. Tofighi-Milani, S. Fattaheian-Dehkordi, M. Gholami, M. Fotuhi-Firuzabad, and M. Lehtonen, "A novel distributed paradigm for energy scheduling of islanded multiagent microgrids," *IEEE Access*, vol. 10, pp. 83636–83649, 2022, doi: [10.1109/ACCESS.2022.3197160](https://doi.org/10.1109/ACCESS.2022.3197160).
- [3] M. Tofighi-Milani, S. Fattaheian-Dehkordi, M. Fotuhi-Firuzabad, and M. Lehtonen, "Decentralized active power management in multi-agent distribution systems considering congestion issue," *IEEE Trans. Smart Grid*, vol. 13, no. 5, pp. 3582–3593, Sep. 2022, doi: [10.1109/TSG.2022.3172757](https://doi.org/10.1109/TSG.2022.3172757).
- [4] A. E. Samani, J. D. M. De Kooning, C. A. U. Blanco, and L. Vandeveld, "Flexible operation strategy for formic acid synthesis providing frequency containment reserve in smart grids," *Int. J. Electr. Power Energy Syst.*, vol. 139, Jul. 2022, Art. no. 107969, doi: [10.1016/j.ijepes.2022.107969](https://doi.org/10.1016/j.ijepes.2022.107969).
- [5] F. Gambou, D. Guilbert, M. Zasadzinski, and H. Rafaralahy, "A comprehensive survey of alkaline electrolyzer modeling: Electrical domain and specific electrolyte conductivity," *Energies*, vol. 15, no. 9, p. 3452, May 2022.
- [6] A. I. Atteya, D. Ali, and N. Sellami, "Precise dynamic modelling of real-world hybrid solar-hydrogen energy systems for grid-connected buildings," *Energies*, vol. 16, no. 14, p. 5449, Jul. 2023.
- [7] M. Tofighi-Milani, S. Fattaheian-Dehkordi, and M. Lehtonen, "Investigating the impact of electrical load types on the frequency response of low inertia power systems," *IEEE Access*, vol. 12, pp. 59771–59781, 2024.
- [8] M. K. Ratib, K. M. Muttaqi, M. R. Islam, D. Sutanto, and A. P. Agalgaonkar, "Electrical circuit modeling of proton exchange membrane electrolyzer: The state-of-the-art, current challenges, and recommendations," *Int. J. Hydrogen Energy*, vol. 49, pp. 625–645, Jan. 2024.
- [9] A. Kishk, "State-of-the-art and technologies in hydrogen production and distribution," M.S. thesis, School Elect. Eng., Aalto Univ., Espoo, Finland, 2023. [Online]. Available: https://scholar.google.com/scholar?hl=en&as_sdt=0%2C5&q=State-of-the-art+and+Technologies+in+Hydrogen+Production+and+Distribution&btnG=
- [10] W. Nicholson, "Account of the new electrical or galvanic apparatus of Sig. Alex. Volta, and experiments performed with the same," *J. Nat. Philos. Chem. Arts*, vol. 4, pp. 179–191, Mar. 1800.
- [11] E. S. Akyüz, E. Telli, and M. Farsak, "Hydrogen generation electrolysers: Paving the way for sustainable energy," *Int. J. Hydrogen Energy*, vol. 81, pp. 1338–1362, Sep. 2024, doi: [10.1016/j.ijhydene.2024.07.175](https://doi.org/10.1016/j.ijhydene.2024.07.175).
- [12] M. B. Hossain, M. R. Islam, K. M. Muttaqi, D. Sutanto, and A. P. Agalgaonkar, "Advancement of fuel cells and electrolysers technologies and their applications to renewable-rich power grids," *J. Energy Storage*, vol. 62, Jun. 2023, Art. no. 106842, doi: [10.1016/j.est.2023.106842](https://doi.org/10.1016/j.est.2023.106842).
- [13] A. Ursúa and P. Sanchis, "Static–dynamic modelling of the electrical behaviour of a commercial advanced alkaline water electrolyzer," *Int. J. Hydrogen Energy*, vol. 37, no. 24, pp. 18598–18614, Dec. 2012.
- [14] A. Buttler and H. Spliethoff, "Current status of water electrolysis for energy storage, grid balancing and sector coupling via power-to-gas and power-to-liquids: A review," *Renew. Sustain. Energy Rev.*, vol. 82, pp. 2440–2454, Feb. 2018.
- [15] M. A. Hossain, M. R. Islam, M. A. Hossain, and M. J. Hossain, "Control strategy review for hydrogen-renewable energy power system," *J. Energy Storage*, vol. 72, Nov. 2023, Art. no. 108170.
- [16] Z. Li, H. Zhang, H. Xu, and J. Xuan, "Advancing the multi-scale understanding on solid oxide electrolysis cells via modelling approaches: A review," *Renew. Sustain. Energy Rev.*, vol. 141, May 2021, Art. no. 110863.

- [17] J. P. Stempien, Q. Sun, and S. H. Chan, "Solid oxide electrolyzer cell modeling: A review," *J. Power Technol.*, vol. 93, no. 4, pp. 216–246, Sep. 2013.
- [18] M. G. Dozein, "System dynamics of low-carbon grids: Fundamentals, challenges, and mitigation solutions," Ph.D. thesis, Dept. Elect. Eng., Univ. Melbourne, Melbourne, VIC, Australia, 2021.
- [19] M. G. Dozein, A. Jalali, and P. Mancarella, "Fast frequency response from utility-scale hydrogen electrolyzers," *IEEE Trans. Sustain. Energy*, vol. 12, no. 3, pp. 1707–1717, Jul. 2021.
- [20] M. G. Dozein, A. M. De Corato, and P. Mancarella, "Virtual inertia response and frequency control ancillary services from hydrogen electrolyzers," *IEEE Trans. Power Syst.*, vol. 38, no. 3, pp. 2447–2459, May 2023.
- [21] S. D. Tavakoli, M. G. Dozein, V. A. Lacerda, M. C. Mañe, E. Prieto-Araujo, P. Mancarella, and O. Gomis-Bellmunt, "Grid-forming services from hydrogen electrolyzers," *IEEE Trans. Sustain. Energy*, vol. 14, no. 4, pp. 2205–2219, Oct. 2023.
- [22] C. Huang, Y. Zong, S. You, and C. Træholt, "Analytical modeling and control of grid-scale alkaline electrolyzer plant for frequency support in wind-dominated electricity-hydrogen systems," *IEEE Trans. Sustain. Energy*, vol. 14, no. 1, pp. 217–232, Jan. 2023.
- [23] M. B. Hossain, M. R. Islam, K. M. Muttaqi, D. Sutanto, and A. P. Agalgaonkar, "Power system dynamic performance analysis based on frequency control by proton exchange membrane electrolyzers," *IEEE Trans. Ind. Appl.*, vol. 59, no. 4, pp. 4998–5008, Jul. 2023.
- [24] M. Agredano-Torres, M. Zhang, L. Söder, and Q. Xu, "Decentralized dynamic power sharing control for frequency regulation using hybrid hydrogen electrolyzer systems," *IEEE Trans. Sustain. Energy*, vol. 15, no. 3, pp. 1847–1858, Jul. 2024.
- [25] M. B. Hossain, M. R. Islam, K. M. Muttaqi, D. Sutanto, and A. P. Agalgaonkar, "Dynamic electrical circuit modeling of a proton exchange membrane electrolyzer for frequency stability, resiliency, and sensitivity analysis in a power grid," *IEEE Trans. Ind. Appl.*, vol. 59, no. 6, pp. 7271–7281, Dec. 2023.
- [26] M. Tofighi-Milani, S. Fattaheian-Dehkordi, and M. Lehtonen, "Dynamic response analysis of alkaline and PEM electrolyzers in low-inertia power systems: A comparative study," in *Proc. IEEE Int. Conf. Environ. Electr. Eng. IEEE Ind. Commercial Power Syst. Eur.*, Jun. 2024, pp. 1–6, doi: [10.1109/EEEIC/ICPSEurope61470.2024.10750998](https://doi.org/10.1109/EEEIC/ICPSEurope61470.2024.10750998).
- [27] C. Henao, K. Agbossou, M. Hammoudi, Y. Dubé, and A. Cardenas, "Simulation tool based on a physics model and an electrical analogy for an alkaline electrolyzer," *J. Power Sources*, vol. 250, pp. 58–67, Mar. 2014.
- [28] D. Guilbert and G. Vitale, "Variable parameters model of a PEM electrolyzer based model reference adaptive system approach," in *Proc. IEEE Int. Conf. Environ. Electr. Eng. IEEE Ind. Commercial Power Syst. Eur. (EEEIC/I&CPS Eur.)*, Jun. 2020, pp. 1–6.
- [29] M. Sánchez, E. Amores, L. Rodríguez, and C. Clemente-Jul, "Semi-empirical model and experimental validation for the performance evaluation of a 15 kW alkaline water electrolyzer," *Int. J. Hydrogen Energy*, vol. 43, no. 45, pp. 20332–20345, Nov. 2018.
- [30] O. Ulleberg, "Modeling of advanced alkaline electrolyzers: A system simulation approach," *Int. J. Hydrogen Energy*, vol. 28, no. 1, pp. 21–33, Jan. 2003.
- [31] R. Yin, L. Sun, A. Khosravi, M. Malekan, and Y. Shi, "Control-oriented dynamic modeling and thermodynamic analysis of solid oxide electrolysis system," *Energy Convers. Manage.*, vol. 271, Nov. 2022, Art. no. 116331.
- [32] D. Guilbert and G. Vitale, "Dynamic emulation of a PEM electrolyzer by time constant based exponential model," *Energies*, vol. 12, no. 4, p. 750, Feb. 2019.
- [33] F. da Costa Lopes and E. H. Watanabe, "Experimental and theoretical development of a PEM electrolyzer model applied to energy storage systems," in *Proc. Brazilian Power Electron. Conf.*, Sep. 2009, pp. 11–15.
- [34] A. A. AlZahrani and I. Dincer, "Thermodynamic and electrochemical analyses of a solid oxide electrolyzer for hydrogen production," *Int. J. Hydrogen Energy*, vol. 42, no. 33, pp. 21404–21413, Aug. 2017.
- [35] K. Motylinski, J. Kupecki, B. Numan, Y. S. Hajimolana, and V. Venkataraman, "Dynamic modelling of reversible solid oxide cells for grid stabilization applications," *Energy Convers. Manage.*, vol. 228, Jan. 2021, Art. no. 113674.
- [36] M. Kolhe and O. Atlam, "Empirical electrical modeling for a proton exchange membrane electrolyzer," in *Proc. Int. Conf. Appl. Supercond. Electromagn. Devices*, Dec. 2011.
- [37] O. Atlam and M. Kolhe, "Equivalent electrical model for a proton exchange membrane (PEM) electrolyser," *Energy Convers. Manage.*, vol. 52, nos. 8–9, pp. 2952–2957, Aug. 2011.
- [38] N. Veerakumar, Z. Ahmad, M. E. Adabi, J. R. Torres, P. Palensky, M. van der Meijden, and F. Gonzalez-Longatt, "Fast active power-frequency support methods by large scale electrolyzers for multi-energy systems," in *Proc. IEEE PES Innov. Smart Grid Technol. Eur. (ISGT-Eur.)*, Oct. 2020, pp. 1–8.
- [39] F. J. Ribeiro, J. A. Peças Lopes, F. J. Soares, and A. G. Madureira, "Hydrogen electrolyser participation in automatic generation control using model predictive control," in *Proc. Int. Conf. Smart Energy Syst. Technol. (SEST)*, Sep. 2024, pp. 1–6, doi: [10.1109/SEST61601.2024.10694041](https://doi.org/10.1109/SEST61601.2024.10694041).
- [40] Á. Hernández-Gómez, V. Ramirez, and D. Guilbert, "Investigation of PEM electrolyzer modeling: Electrical domain, efficiency, and specific energy consumption," *Int. J. Hydrogen Energy*, vol. 45, no. 29, pp. 14625–14639, May 2020.
- [41] M. T. de Groot, J. Kraakman, and R. L. G. Barros, "Optimal operating parameters for advanced alkaline water electrolysis," *Int. J. Hydrogen Energy*, vol. 47, no. 82, pp. 34773–34783, Sep. 2022.
- [42] A. Tabanjat, M. Becherif, M. Emziane, D. Hissel, H. S. Ramadan, and B. Mahmah, "Fuzzy logic-based water heating control methodology for the efficiency enhancement of hybrid PV-PEM electrolyser systems," *Int. J. Hydrogen Energy*, vol. 40, no. 5, pp. 2149–2161, Feb. 2015, doi: [10.1016/j.ijhydene.2014.11.135](https://doi.org/10.1016/j.ijhydene.2014.11.135).
- [43] X. Wang, X. Meng, G. Nie, B. Li, H. Yang, and M. He, "Optimization of hydrogen production in multi-electrolyzer systems: A novel control strategy for enhanced renewable energy utilization and electrolyzer lifespan," *Appl. Energy*, vol. 376, Dec. 2024, Art. no. 124299, doi: [10.1016/j.apenergy.2024.124299](https://doi.org/10.1016/j.apenergy.2024.124299).
- [44] J. Mao, Z. Li, J. Xuan, X. Du, M. Ni, and L. Xing, "A review of control strategies for proton exchange membrane (PEM) fuel cells and water electrolyzers: From automation to autonomy," *Energy AI*, vol. 17, Sep. 2024, Art. no. 100406, doi: [10.1016/j.egyai.2024.100406](https://doi.org/10.1016/j.egyai.2024.100406).
- [45] R. Phillips, A. Edwards, B. Rome, D. R. Jones, and C. W. Dunnill, "Minimising the ohmic resistance of an alkaline electrolysis cell through effective cell design," *Int. J. Hydrogen Energy*, vol. 42, no. 38, pp. 23986–23994, Sep. 2017.
- [46] J. Raj and S. R. Rajasree, "A microgrid with hybrid solar-fuel cell system with CHP application," in *Proc. IEEE 2nd Int. Conf. Sustain. Energy Future Electr. Transp. (SeFeT)*, Aug. 2022, pp. 1–6.
- [47] V. Ram, Infantraj, and S. R. Salkuti, "Modelling and simulation of a hydrogen-based hybrid energy storage system with a switching algorithm," *World Electr. Vehicle J.*, vol. 13, no. 10, p. 188, Oct. 2022.
- [48] M. B. Hossain, M. R. Islam, K. M. Muttaqi, D. Sutanto, and A. P. Agalgaonkar, "Modeling and performance analysis of renewable energy hub connected to an AC/DC hybrid microgrid," *Int. J. Hydrogen Energy*, vol. 47, no. 66, pp. 28626–28644, Aug. 2022.
- [49] Y.-P. Xu, Z.-H. Lin, T.-X. Ma, C. She, S.-M. Xing, L.-Y. Qi, S. G. Farkoush, and J. Pan, "Optimization of a biomass-driven Rankine cycle integrated with multi-effect desalination, and solid oxide electrolyzer for power, hydrogen, and freshwater production," *Desalination*, vol. 525, Mar. 2022, Art. no. 115486.
- [50] I. Vincent and D. Bessarabov, "Low cost hydrogen production by anion exchange membrane electrolysis: A review," *Renew. Sustain. Energy Rev.*, vol. 81, pp. 1690–1704, Jan. 2018.
- [51] R. Bhandari, C. A. Trudewind, and P. Zapp, "Life cycle assessment of hydrogen production via electrolysis—A review," *J. Clean. Prod.*, vol. 85, pp. 151–163, Mar. 2014.
- [52] A. Ursua, L. M. Gandia, and P. Sanchis, "Hydrogen production from water electrolysis: Current status and future trends," *Proc. IEEE*, vol. 100, no. 2, pp. 410–426, Feb. 2012.
- [53] O. Faye, J. Szpunar, and U. Eduok, "A critical review on the current technologies for the generation, storage, and transportation of hydrogen," *Int. J. Hydrogen Energy*, vol. 47, no. 29, pp. 13771–13802, Apr. 2022.
- [54] M. Carmo, D. Fritz, J. Mergel, and D. Stolten, "A comprehensive review on PEM water electrolysis," *Int. J. Hydrog. Energy*, vol. 38, no. 12, pp. 4901–4934, Mar. 2013.
- [55] G. Flis and G. Wakim, "Solid oxide electrolysis: A technology status assessment," Clean Air Task Force (CATF), Boston, MA, USA, Tech. Rep., 2023. [Online]. Available: <https://cdn.catf.us/wp-content/uploads/2023/11/15092028/solid-oxide-electrolysis-report.pdf>
- [56] Y. Xia, H. Cheng, H. He, and W. Wei, "Efficiency and consistency enhancement for alkaline electrolyzers driven by renewable energy sources," *Commun. Eng.*, vol. 2, no. 1, p. 22, May 2023, doi: [10.1038/s44172-023-00070-7](https://doi.org/10.1038/s44172-023-00070-7).

- [57] IEA. (2019). *The Future of Hydrogen*. [Online]. Available: <https://www.iea.org/reports/the-future-of-hydrogen>
- [58] X. Wei, S. Sharma, A. Waeber, D. Wen, S. N. Sampathkumar, M. Margni, F. Maréchal, and J. Van Herle, "Comparative life cycle analysis of electrolyzer technologies for hydrogen production: Manufacturing and operations," *Joule*, vol. 8, no. 12, pp. 3347–3372, Dec. 2024.
- [59] S. A. Grigoriev, V. N. Fateev, D. G. Bessarabov, and P. Millet, "Current status, research trends, and challenges in water electrolysis science and technology," *Int. J. Hydrogen Energy*, vol. 45, no. 49, pp. 26036–26058, Oct. 2020, doi: [10.1016/j.ijhydene.2020.03.109](https://doi.org/10.1016/j.ijhydene.2020.03.109).
- [60] A. S. Tijani and A. Rahim, "Numerical modeling the effect of operating variables on Faraday efficiency in PEM electrolyzer," in *Proc. 3rd Int. Conf. Syst.-Integr. Intell. New Chall. Prod. Prod. Eng.*, vol. 26, Jan. 2016, pp. 419–427, doi: [10.1016/j.protcy.2016.08.054](https://doi.org/10.1016/j.protcy.2016.08.054).
- [61] Z. Shangguan, H. Li, B. Yang, Z. Zhao, T. Wang, L. Jin, and C. Zhang, "Optimization of alkaline electrolyzer operation in renewable energy power systems: A universal modeling approach for enhanced hydrogen production efficiency and cost-effectiveness," *Int. J. Hydrogen Energy*, vol. 49, pp. 943–954, Jan. 2024, doi: [10.1016/j.ijhydene.2023.10.057](https://doi.org/10.1016/j.ijhydene.2023.10.057).
- [62] M. Chen, J. Jia, B. Zhang, L. Han, M. Ji, Z. Yu, D. Li, W. Wang, H. Jia, and H. Xu, "Enhancing the efficiency of multi-electrolyzer clusters with lye mixer: Topology design and control strategy," *Energy Eng.*, vol. 121, no. 10, pp. 3055–3074, 2024.
- [63] S. W. Sharshir, A. Joseph, M. M. Elsayad, A. A. Tareemi, A. W. Kandeal, and M. R. Elkadeem, "A review of recent advances in alkaline electrolyzer for green hydrogen production: Performance improvement and applications," *Int. J. Hydrogen Energy*, vol. 49, pp. 458–488, Jan. 2024.
- [64] X. Lu, B. Du, S. Zhou, W. Zhu, Y. Li, Y. Yang, C. Xie, B. Zhao, L. Zhang, J. Song, and Z. Deng, "Optimization of power allocation for wind-hydrogen system multi-stack PEM water electrolyzer considering degradation conditions," *Int. J. Hydrogen Energy*, vol. 48, no. 15, pp. 5850–5872, Feb. 2023.
- [65] M. Ehmer and F. Khan, "A comparative study of white box, black box and grey box testing techniques," *Int. J. Adv. Comput. Sci. Appl.*, vol. 3, no. 6, pp. 1–11, 2012.
- [66] M. A. F. Strauss, "Comparison of cell and stack concepts for the alkaline water electrolysis and their influence on the voltage efficiency and current density," M.S. thesis, Brandenburg Univ. Technol. Cottbus Senftenberg, Cottbus, Germany, 2021. [Online]. Available: https://scholar.google.com/scholar?hl=en&as_sdt=0%2C5&q=Comparison+of+cell+and+stack+concepts+for+the+alkaline+water+electrolysis+and+their+influence+on+the+voltage+efficiency+and+current+density.&btnG=
- [67] J. Dang, F. Yang, Y. Li, Y. Zhao, M. Ouyang, and S. Hu, "Experiments and microsimulation of high-pressure single-cell PEM electrolyzer," *Appl. Energy*, vol. 321, Sep. 2022, Art. no. 119351, doi: [10.1016/j.apenergy.2022.119351](https://doi.org/10.1016/j.apenergy.2022.119351).
- [68] D.-J. Lee and L. Wang, "Small-signal stability analysis of an autonomous hybrid renewable energy power generation/energy storage system Part I: Time-domain simulations," *IEEE Trans. Energy Convers.*, vol. 23, no. 1, pp. 311–320, Mar. 2008.
- [69] J. Eichman, K. Harrison, and M. Peters, "Novel electrolyzer applications: Providing more than just hydrogen," Nat. Renew. Energy Lab. (NREL), Golden, CO, USA, Tech. Rep. NREL/TP-5400-61758, 2014. [Online]. Available: <https://www.nrel.gov/docs/fy14osti/61758.pdf>
- [70] M. K. Ratiib, S. Alkhalaf, T. Senjyu, A. Rashwan, M. M. Mahmoud, A. M. Hemeida, and D. Osheba, "Applications of hybrid model predictive control with computational burden reduction for electric drives fed by 3-phase inverter," *Ain Shams Eng. J.*, vol. 14, no. 8, Aug. 2023, Art. no. 102028.
- [71] F. Fouda-Onana, M. Chandresris, V. Médeau, S. Chelghoum, D. Thoby, and N. Guillet, "Investigation on the degradation of MEAs for PEM water electrolyzers part I: Effects of testing conditions on MEA performances and membrane properties," *Int. J. Hydrogen Energy*, vol. 41, no. 38, pp. 16627–16636, Oct. 2016, doi: [10.1016/j.ijhydene.2016.07.125](https://doi.org/10.1016/j.ijhydene.2016.07.125).
- [72] R. Cozzolino and G. Bella, "A review of electrolyzer-based systems providing grid ancillary services: Current status, market, challenges and future directions," *Frontiers Energy Res.*, vol. 12, Feb. 2024, Art. no. 1358333.
- [73] A. Escamilla, D. Sánchez, and L. García-Rodríguez, "Assessment of power-to-power renewable energy storage based on the smart integration of hydrogen and micro gas turbine technologies," *Int. J. Hydrogen Energy*, vol. 47, no. 40, pp. 17505–17525, May 2022, doi: [10.1016/j.ijhydene.2022.03.238](https://doi.org/10.1016/j.ijhydene.2022.03.238).



MAHYAR TOFIGHI-MILANI (Student Member, IEEE) received the B.Sc. degree in electrical engineering from Iran University of Science and Technology (IUST), in 2018, and the M.Sc. degree in electrical engineering from the Sharif University of Technology in 2021. He is currently pursuing the Ph.D. with the Department of Electrical Engineering and Automation, Aalto university. His research interests include smart grids, electricity markets, renewable and distributed energy resources, microgrids, frequency dynamics, and low-inertia power systems.



SAJJAD FATTAHEIAN-DEHKORDI (Member, IEEE) received the B.Sc. degree in electrical and computer engineering from the University of Tehran, in 2012, the M.Sc. degree in electrical engineering and power systems from the Sharif University of Technology, in 2014, and the Ph.D. degree from Aalto University, Espoo, Finland, in 2023. His research interests include power systems planning, operations, and economics, with a focus on issues relating with the integration of renewable energy resources into the systems.



MATTI LEHTONEN received the master's and Licentiate degrees in electrical engineering from the Helsinki University of Technology, in 1984 and 1989, respectively, and the Doctor of Technology degree from the Tampere University of Technology, in 1992. He has been a Professor with the Helsinki University of Technology (now Aalto University), where he is the Head of power systems and high voltage engineering. His main research interests include power system planning and asset management and power system protection, including earth fault problems, harmonic related issues, and applications of information technology in distribution systems.

...